Superconductivity of Metallic Boron in MgB$_2$

J. Kortus,[1,2,*] I. I. Mazin,[2] K. D. Belashchenko,[3] V. P. Antropov,[3] and L. L. Boyer[2]

[1]*Georgetown University, Washington, D.C. 20057*
[2]*Center for Computational Materials Science, Code 6390, Naval Research Laboratory, Washington, D.C. 20375*
[3]*Ames Laboratory, ISU, Ames, Iowa 50011*
(Received 29 January 2001)

Boron in MgB$_2$ forms stacks of honeycomb layers with magnesium as a space filler. Band structure calculations indicate that Mg is substantially ionized, and the bands at the Fermi level derive mainly from B orbitals. Strong bonding with an ionic component and considerable metallic density of states yield a sizable electron-phonon coupling. Together with high phonon frequencies, which we estimate via zone-center frozen phonon calculations to be between 300 and 700 cm^{-1}, this produces a high critical temperature, consistent with recent experiments. Thus MgB$_2$ can be viewed as an analog of the long sought, but still hypothetical, superconducting metallic hydrogen.

Before the discovery of high-temperature superconductors much effort was devoted to boosting the critical temperature of conventional, BCS-Eliashberg superconductors [1]. An exotic and appealing idea going back to the early 1960's was that of metallic hydrogen [2]. The arguments were very simple: due to the light mass, the phonon frequencies in metallic hydrogen would be very high, of the order of several thousand degrees Kelvin, and the prefactor in the BCS formula would be very large, so that even a moderate coupling constant would provide a sizable T_c. This idea can be quantified as follows: for monatomic solids, the electron-phonon coupling (EPC) constant, λ, which enters the BCS equation, can be written in the so-called McMillan-Hopfield form [3], $\lambda = N(0)\langle I^2\rangle/M\langle\omega^2\rangle$, where $N(0)$ is the density of states (DOS) at the Fermi level per spin per atom, $\langle I^2\rangle$ is the properly averaged electron-ion matrix element squared, M is the atomic mass, and $\langle\omega^2\rangle$ is (again, properly averaged) the phonon frequency. The product $M\langle\omega^2\rangle$ does not depend on the mass, but on the force constants only [1], while $\eta = N(0)\langle I^2\rangle$, also known as the Hopfield factor, is a purely electronic property. Correspondingly, light elements, everything else being the same, are beneficial for superconductivity.

Lacking metallic hydrogen, attention was focused upon compounds with light elements: carbides, nitrides (arguably, the superconductivity in fullerenes was a discovery along this road). Indeed, many of them were "high-T_c superconductors" on the contemporary scale: 10–15 K. It was pointed out [4] that $\langle I^2\rangle$ is rather large in these materials due to the relatively high ionicity (although not as high as in MgB$_2$), but $N(0)$ is rather small. This led to the suggestion of cubic MoN, which would have a larger $N(0)$ than existing nitrides and carbides, as a hypothetical superconductor with $T_c > 30$ K [5].

The recently discovered medium-T_c superconductor MgB$_2$ [6] with $T_c \gtrsim 39$ K is clearly a continuation of the same idea. The main component, B, is even lighter than C and N. Furthermore, electronic structure calculations show that the compound is not only quite ionic with a siz-

able DOS, but also has strong covalent B-B bonding (the bonding-antibonding splitting due to in-plane B-B hopping is about 6 eV) and thus exhibits strong electron-phonon interactions. Interestingly, unlike carbides and nitrides, and similar to metallic hydrogen, electrons at the Fermi level (and below) are predominantly B like. Mg s states are pushed up by the B p_z orbitals and fully donate their electrons to the boron-derived conduction bands. In the following we will describe the physics of such "metallic" boron in detail, present an estimate of the EPC constant, and propose some routes for optimizing T_c in this kind of compound.

MgB$_2$ occurs in the so-called AlB$_2$ structure. Borons form a primitive honeycomb lattice, consisting of graphite-type sheets stacked with no displacement. The borons form hexagonal prisms with the base diameter of 3.5 Å nearly equal to the height. This creates large, nearly spherical pores for Mg. As in graphite, the intraplanar B-B bonds are much shorter than the distance between the planes, and hence the B-B bonding is strongly anisotropic. However, the interplane bonds are only twice as long as the intraplane ones, as compared to the ratio of 2.4 in graphite, allowing for a significant interplane hopping.

We have calculated the electronic structure of MgB$_2$ using a general potential LAPW code [7]. For the rigid atomic spheres calculations we used the Stuttgart LMTO code [8]. For the exchange-correlation potential, the generalized gradient approximation of Ref. [9] was employed. Despite the rather simple crystal structure, very few electronic structure calculations for MgB$_2$ have been reported (a model TB calculation of Burdett and Miller [10] and a recent full-potential LMTO study [11]), and these have concentrated mainly on chemical bonding, paying hardly any attention to transport and electronic properties. The results of our LAPW calculations are shown in Figs. 1 and 2. We note first that there is almost no valence charge inside the Mg muffin-tin (MT) sphere (less than $0.2e$). About half of the total valence charge resides inside the B spheres, and about the same amount in the interstitials. This is partially due to the fact that the chosen LAPW setup employs
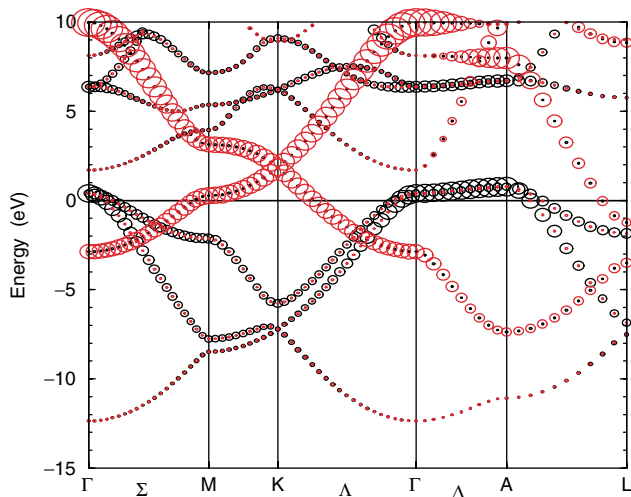
FIG. 1 (color).   Band structure of MgB_2 with the B p character. The radii of the red (black) circles are proportional to the B p_z (B $p_{x,y}$) character.

rather small MT spheres for Mg. For the LMTO calculations we used an atomic sphere of nearly the size of the free Mg atom (up to $3.13a_B$), and obtained, as expected, a larger charge of 2.8 electrons. However less than 25% of the charge has s character. The remaining charge of p, d, and f character arises not from Mg electrons but rather from the tails of the B p orbitals and contributions from the interstitials. In fact, one can say that Mg is fully ionized in this compound, however the electrons donated to the system are not localized on the anion, but rather are distributed over the whole crystal.

The resulting band structure can be easily understood in terms of the boron sublattice. The character of the bands is plotted in Fig. 1. We show only the B p character, since other contributions near the Fermi level are very small. Observe two B band systems: two bands are derived from
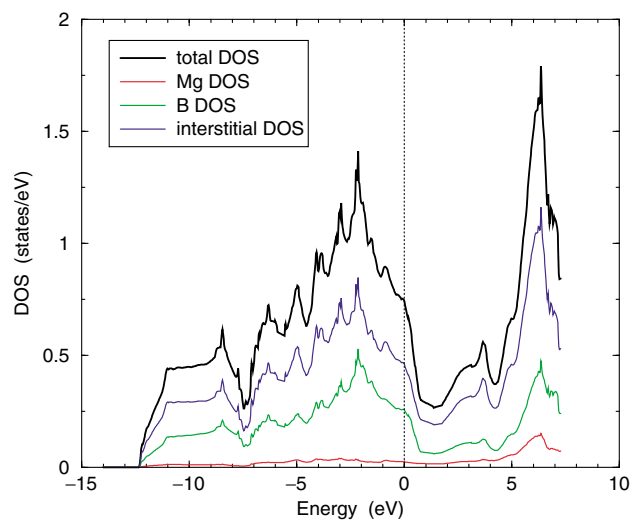
B p_z states and four from B $p_{x,y}$. All these bands are highly dispersive (light), the former being quite isotropic and the latter more two dimensional. Both p_z bands cross the Fermi level (in different parts of the Brillouin zone), but only two bonding $p_{x,y}$ bands do so, and only near the Γ point. They form two small cylindrical Fermi surfaces around the Γ-A line (Fig. 3). However, due to their 2D character, they contribute more than 30% to the total $N(0)$.

In contrast, the p_z bands have 3D character, since the smaller intraplane distance compensates for a smaller ($pp\pi$ vs $pp\sigma$) hopping. In the nearest neighbor tight binding (TB) model their dispersion is $\varepsilon_{\mathbf{k}} = \varepsilon_0 + 2t_{pp\sigma} \times \cos ck_z \pm t_{pp\pi}\sqrt{3 + 2\cos\mathbf{a}_1\mathbf{k} + 2\cos\mathbf{a}_2\mathbf{k} + 2\cos\mathbf{a}_3\mathbf{k}}$ where $\mathbf{a}_{1,2,3}$ are the smallest in-plane lattice vectors. The on-site parameter ε_0 can be found from the eigenvalue at the K point and is $\sim$1.5 eV above the Fermi energy. We estimated $t_{pp\sigma}$ and $t_{pp\pi}$ from the LMTO calculations as $\sim$2.5 and $\sim$1.5 eV, respectively. This model gives a very good description of the p_z band structure near and below the Fermi level, although the antibonding band acquires some additional dispersion by hybridizing with the Mg p band. The role of Mg in forming this band structure can be elucidated by removing the Mg atoms from the lattice entirely and repeating the calculations in this hypothetical structure. The in-plane dispersion of both sets of bands at and below the Fermi level changes very little ($pp\pi$ bands are hardly changed, while the $pp\sigma$ in-plane dispersion changes by $\sim$10%). The k_z dispersion of the p_z bands is increased in MgB_2 as compared with the hypothetical empty B_2 lattice by about 30%, and these bands shift down with respect to the $p_{x,y}$ bands by approximately 1 eV. This shift, as well as the additional dispersion, comes mainly from the hybridization with the empty Mg s band, which is correspondingly pushed further up, increasing the effective ionicity. Substantial k_z dispersion of the p_z bands

FIG. 2 (color).   Total density of states (DOS) and partial DOS for the MgB_2 compound. The small Mg DOS is partially due to the small r_{MT} of $1.8a_B$ used.
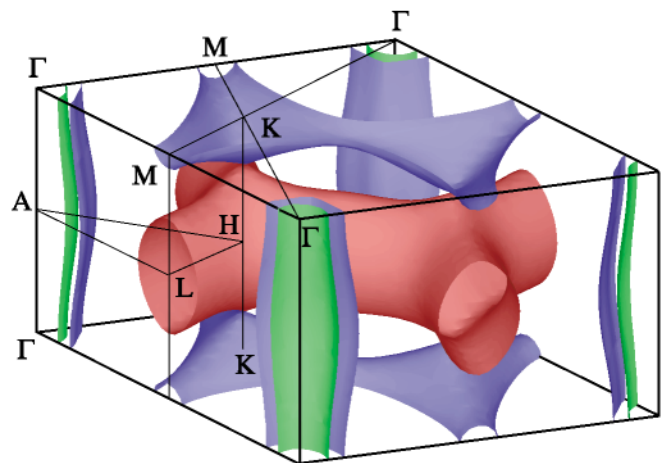

FIG. 3 (color).   The Fermi surface of MgB_2. Green and blue cylinders (holelike) come from the bonding $p_{x,y}$ bands, the blue tubular network (holelike) from the bonding p_z bands, and the red (electronlike) tubular network from the antibonding p_z band. The last two surfaces touch at the K point.

produces the Fermi surface which is approximately mirror reflected with respect to a plane between the $k_z = 0$ and $k_z = \pi/c$ planes, one pocket (electronlike) coming from the antibonding and the other (holelike) from the bonding p_z band. The two surfaces touch at one point on the K-H line and form a honeycomb tubular network, replicating in reciprocal space the boron lattice in real space.

The resulting bands are fairly 3D: the average Fermi velocities are $v_{x,y} = 4.90 \times 10^7$ cm/s and $v_z = 4.76 \times 10^7$ cm/s. The plasma frequencies are $\omega_{px,y} = 7.1$ eV and $\omega_{pz} = 6.9$ eV. Correspondingly, we predict fairly isotropic high-temperature electrical resistivity, with the linear slope $d\rho/dT \approx 0.08\lambda_{\mathrm{tr}}$ $\mu\Omega$ cm/K. The total DOS at the Fermi level is $N(0) = 0.36$ states/spin f.u.

The above described band structure is typical for an sp metal. What is *not* typical is that this particular sp metal is held together by covalent bonding with a substantial ionic component [12], which inevitably leads to a strong electron-phonon interaction. In the following we present a semiquantitative estimate of the corresponding coupling constant, and argue that the fortunate combination of strong bonding, sizable $N(0)$, and high phonon frequency is responsible for the high transition temperature in this compound.

In its most rigorous formulation the McMillan-Hopfield formula reads [1]

$$\lambda = n^{-1} \sum_{ij} \langle N I_{i\alpha} I_{j\beta}\rangle (\Phi^{-1})_{i\alpha,j\beta}, \qquad (1)$$

where the indices i, j run over all n ions in the crystal; α, β are Cartesian indices; $\langle N I_{i\alpha} I_{j\beta}\rangle$ is the electron-ion matrix element averaged over the Fermi surface; and $\Phi_{i\alpha,j\beta}$ is the standard force matrix. While this expression is exact, a number of simplifications are needed to make it more practical. One usually neglects the nondiagonal terms and reduces Eq. (1) to one unit cell. The standard justification makes use of the large size of the Fermi surface; see Ref. [1]:

$$\lambda \approx \sum_i \langle N I^2\rangle_i \Phi_{ii}^{-1} = \sum_i \eta_i (\Phi_{ii})^{-1}. \qquad (2)$$

The quantity $\Phi_{ii} = \partial^2 E_{\mathrm{tot}} \partial R_i^2$ is a local quantity, which can be calculated from the total energy differences of frozen zone-center phonons. The Hopfield factor can be calculated in the rigid muffin-tin (or rigid atomic sphere) approximation [13] (RMTA), assuming that the change of the crystal potential due to an ion's displacement can be described by shifting the electronic charge distribution rigidly inside the

TABLE I. Partial LMTO DOS, $N(0)$, in eV^{-1}/spin and partial Hopfield factors, η, in mRy/a_B^2, for Mg and B (per atom).

| l | \multicolumn{4}{c}{$N(0)$} | \multicolumn{3}{c}{η} |
	s	p	d	f	sp	pd	df
Mg	0.018	0.043	0.078	0.019	<1	2	3
B	0.003	0.199	0.010	$\cdots$	<1	135	$\cdots$

corresponding atomic sphere. Although expressions for η have been derived for arbitrary site symmetry [14], these are complicated and we will use here simplified formulas [13] formally correct for cubic site symmetry. Then η can be readily calculated from the LMTO potential parameters and partial DOS's. We show the results in Table I.

In order to get an estimate of the phonon spectrum of the system, we calculated all zone-center modes, using the full-potential LAPW method. There are four distinct modes [15]: one silent mode, B_{1g} (two borons displaced along z in opposite directions), one doubly degenerate Raman mode, E_{2g} (in-plane displacements of borons), and two infrared-active modes, which do not involve changes of in-plane bonds: A_{2u} (B and Mg planes moving against each other), and a doubly degenerate E_{1u} mode (B and Mg planes sliding along x, y). Their frequencies are, respectively, 690, 515, 390, and 320 cm^{-1}, and their force constants are 390, 220, 70, and 44 mRy/a_B^2/atom. All calculations were carried out at the experimental lattice constant and c/a ratio [16]. The E_{2g} mode shows strong anharmonicity. While the harmonic frequency calculated from the second derivative of the total energy with respect to the phonon coordinate yields 515 cm^{-1}, a numeric solution for the calculated anharmonic potential results in an anharmonic frequency of 590 cm^{-1}.

Given the physics of the electronic structure described above, it seems likely that the lowest mode couples little with the electrons and that its softness is derived from its in-plane acoustic character. Thus, we excluded it from the calculations of λ below. Correspondingly, the average inverse force matrix for boron is $(\Phi_B)^{-1} = M_B^{-1}\langle\omega^{-2}\rangle = 7.1a_B^2$/Ry, corresponding to $\langle\omega^{-2}\rangle^{-1/2} \approx 400$ cm^{-1}. Together with the above value for η this gives $\lambda \approx 0.7$ and the logarithmically averaged frequency of the same three modes is $(690 \times 515^2 \times 390)^{0.25} = \langle\omega_{\log}\rangle \approx 500$ cm$^{-1} \approx 700$ K. We can now estimate the critical temperature according to the McMillan formula, $T_c = \frac{\langle\omega_{\log}\rangle}{1.2} \exp[-1.02(1 + \lambda)/(\lambda - \mu^* - \mu^*\lambda)]$. Using for the Coulomb pseudopotential μ^* the commonly accepted value 0.1, we obtain $T_c \approx 22$ K.

TABLE II. Comparison of the electron-phonon coupling in Al and in MgB$_2$. The entries labeled by a question mark are obtained by scaling the RMTA λ by the ratio of $\lambda_{\exp}/\lambda_{\mathrm{rmt}}$ in Al. q_{TF} is the Thomas-Fermi screening parameter in a_B^{-1}. T_c was calculated by the McMillan formula with $\mu^* = 0.1$. LAPW $N(0)$ is given in eV^{-1}/spin, η in mRy/a_B^2, and $\langle M\omega^2\rangle$ in Ry/a_B^2.

	$N(0)$	η_{rmt}	$\langle\omega_{\log}\rangle$	$\langle M\omega^2\rangle$	λ_{rmt}	$T_c(\lambda_{\mathrm{rmt}})$	$\lambda_{\exp}$	$T_c(\lambda_{\exp})$	$T_{c,\exp}$	q_{TF}
Al	0.15	27	250	0.135	0.2	0	0.4	1.3	1.3	0.73
MgB$_2$	0.18 (per B)	135	500	0.141	0.7	22	1.4?	70?	39	0.70

It is instructive to compare the calculation above with a typical sp superconductor, Al (Table II). RMTA usually underestimates the electron-ion scattering in sp metals due to the weaker screening than in d metals. Also in Al, λ is underestimated by a factor of 2. The screening properties of MgB_2 are similar to those of Al (they have similar Thomas-Fermi screening lengths), and the electronic properties are similar as well. It is therefore tempting to scale the calculated λ for MgB_2 by the same factor. The scaled results are also shown in Table II and the corresponding T_c is approximately 70 K. Let us emphasize that these numbers should be regarded only as rough estimates. The RMTA in MgB_2 is clearly a worse approximation than in Al. The boron site symmetry is far from cubic and, moreover, large differences in the atomic sphere radii lead to artificial potential jumps at the sphere boundary, a problem for which there is no remedy in RMTA. In other words, with regard to EPC, our calculations should be considered as a qualitative indication of a strong electron-phonon interaction. We can nevertheless be confident of our main qualitative conclusions.

Our main conclusion is that MgB_2, being essentially metallic boron held together by covalent B-B and ionic B-Mg bonding, is electronically a typical sp metal with a typical DOS. Strong bonding induces strong electron-ion scattering and hence strong electron-phonon coupling. An additional benefit is the high frequency of the boron vibrations (while the force constants remain reasonably soft). Superconductivity is mainly due to boron. The light mass and correspondingly large zero-point vibrations ($>0.1a_B$) suggest a possibility of anharmonic and/or nonlinear EPC, and possible deviation of the isotope effect from 100%. Isovalent doping may be beneficial if it increases the density of states $N(0)$. Lattice expansion due to Ca doping should lead to an overall increase of the density of states, and may provide the additional benefit of reduced p_z-s-p_z hopping. Another interesting dopant is Na, which should not only expand the lattice, but also decrease the Fermi level, exposing more of the $p_{x,y}$ bands, which may provide an additional contribution to λ.

Finally, let us outline the directions for further theoretical investigation. First, EPC calculations beyond the RMTA (e.g., in the linear response formalism) are highly desirable and computationally feasible. Second, calculations with full structure optimization for (hypothetical) CaB_2 and BeB_2, and virtual crystal calculations for Na doping should elucidate the effect of isovalent and hole doping, giving some hints toward further optimizing T_c. Work along these lines is currently in progress.

Note added.— Since this paper was submitted, a sizable, but incomplete, isotope shift for B [17] (but not for Mg) was obtained, supporting the picture described above.

*Current address: MPI für Festkörperforschung, Postfach 80065, D-70506 Stuttgart, Germany.

[1] *The Problem of High Temperature Superconductivity,* edited by V. L. Ginzburg and D. A. Kirzhnits (Consultant Bureau, New York, 1982).

[2] B. Adler, in *Progress in Very High Pressure Research,* edited by T. Bundy (Wiley, New York, 1960); N. Ashcroft, Phys. Rev. Lett. **21**, 1748 (1968).

[3] W. L. McMillan, Phys. Rev. **167**, 331 (1968).

[4] B. M. Klein and D. A. Papaconstantopulos, Phys. Rev. Lett. **32**, 1193 (1974).

[5] D. A. Papaconstantopulos *et al.,* Nature (London) **308**, 494 (1984).

[6] J. Nagamatsu *et al.,* Nature (London) **410**, 63 (2001).

[7] P. Blaha, K. Schwarz, and J. Luitz, computer code WIEN97, Vienna University of Technology, Vienna, 1997. Improved and updated of original code published by B. Blaha, K. Schwarz, P. Sorantin, and S. B. Trickey, Comput. Phys. Commun. **59**, 399 (1990). We used for all calculations $r_{MT} \times k_{max} = 8.0$, $l_{max} = 10$, and $G_{max} = 20$, r_{MT} Mg 1.8 and B $1.5a_B$.

[8] We used two different LMTO setups throughout this work. One was carefully selected to reproduce the full-potential LAPW results near the Fermi surface nearly exactly, and was used essentially as a tool for interpolating the LAPW bands. The relevant parameters were $r_{Mg} = 3.13$, $r_B = 2.01$. The other was produced by the *lmhart* program (part of the Stuttgart TB-LMTO 4.7 package) which selects the sphere so as to minimize discontinuity in the Hartree potential ($r_{Mg} = 3.23$, $r_B = 1.87$). The latter is more physical and was used for the EPC calculations. Because of the large Mg sphere, it is important to include f states on Mg, and to perform the final run with the linearization parameters E_ν set to the Fermi level.

[9] J. P. Perdew and Y. Wang, Phys. Rev. B **45**, 13244 (1992).

[10] J. K. Burdett and G. J. Miller, Chem. Mater. **2**, 12 (1989).

[11] A. I. Ivanovskii and N. I. Medvedeva, Russ. J. Inorg. Chem. **45**, 1234 (2000).

[12] More detailed discussion of bonding in MgB_2 can be found in K. D. Belashchenko, M. van Schilfgaarde, and V. P. Antropov, cond-mat/0102290.

[13] G. Gaspari and B. Gyorffy, Phys. Rev. Lett. **28**, 801 (1972).

[14] I. I. Mazin, S. N. Rashkeev, and S. Y. Savrasov, Phys. Rev. B **42**, 366 (1990).

[15] H. T. Stokes and D. M. Hatch, *Isotropy Subgroups of the 230 Crystallographic Space Groups* (World Scientific, Singapore, 1988).

[16] $a = 3.083$ Å, $c/a = 1.142$; A. Lipp and M. Roder, Z. Anorg. Allg. Chem. **344**, 225 (1966). Calculated numbers differ from these by -0.4 and 0.6%, respectively.

[17] S. L. Bud'ko *et al.,* Phys. Rev. Lett. **86**, 1877 (2001).